Available online at www.sciencedirect.com
ScienceDirect
Thin Solid Films 516 (2008) 4258–4266
www.elsevier.com/locate/tsf

Chemical formation of palladium-free surface-nickelized polyimide film for flexible electronics

Yu-Sheng Hsiao [a], Wha-Tzong Whang [a,*], Sheng-Chang Wu [b], Kuen-Ru Chuang [b]

[a] *Department of Materials Science and Engineering, National Chiao Tung University, HsiuChu 300, Taiwan, ROC*
[b] *Taimide Technology Company, Taiwan, ROC*

Received 10 January 2007; received in revised form 9 December 2007; accepted 29 December 2007
Available online 15 January 2008

Abstract

Flexible polyimide (PI) films for flexible electronics were surface-nickelized using a fully solution-based process and excellent adhesion between the nickel and polyimide phases was observed. Polyimide substrates were modified by alkaline hydrolysis, ion exchange, reduction and nickel electroless deposition without palladium. Atomic force microscopy and field emission scanning electron microscopy were used to follow the growth of nickel nanoparticles (Ni-NPs) and nickel layers on the polyimide surface. The surface resistances of the Ni-NPs/PI films and Ni/PI films, measured using a four-point probe, were 1.6×10^7 and 0.83 Ω/cm^2, respectively. The thicknesses of Ni-NPs and the Ni layer on the polyimide surface were 82 nm and 382 nm, respectively, as determined by transmission electron microscopy, and the Ni layer adhered well to PI, as determined by the adhesive tape testing method.

Keywords: Flexible electronics; Polyimide; Nickel electroless deposition

1. Introduction

Flexible aromatic polyimide (PI) films have been widely applied in soft electronics and microelectronics packages. The base materials of flexible printed circuits (FPC) and other soft electronics are copper on polyimide with or without adhesive. The former is called the three-layer mode (metal/adhesive/PI), while the latter is the two-layer mode (metal/PI). The development of FPC with smaller line widths and increased wire density is based on the two-layer mode. Several fabrication methods have been applied to the two-layer system. Popular methods are coating Poly(amic acid) (PAA) onto a copper surface; press a copper layer onto PI at high-temperature, or sputtering a copper thin layer on PI followed by electrochemical copper plating. However, these methods raise problems. For instance, in the coating adhesive PAA method, the product warps after imidization. In the pressing copper layer and sputtering copper methods, the adhesion is weak at the interface between the copper and PI [1–3]. Although other methods for sputtering copper use apply plasma to increase the roughness to improve adhesion, another problem is that such approaches must be implemented in high vacuum systems, increasing the complexity of the process [4–9].

Recently, the two-layer mode (metal/PI) has been modified by using alkaline hydrolysis to open imide rings, followed by ion exchange with metal ions and the reduction of copper ions on PI [10–18]. Alkali treatments in the first step have been investigated using an aqueous solution of NaOH and KOH [19–22]. The ion exchange rate of copper and the dispersion of copper in underlying modified PI in the second step have been widely discussed [12,14–16]. In the third step, the methods for reducing copper involve a thermally-induced hydrogen reaction, an ultraviolet (UV)-light-induced photochemical reaction (TiO_2 as photocatalysts) and a chemical reaction (dimethylamine borane (DMAB) and sodium borohydride ($NaBH_4$) as reductants) [12,14–16]. On hydrogen-induced systems, high-temperature treatment raises problems of diffusion and oxidation of the Cu nanoparticles. In ultraviolet (UV)-light-induced systems and chemical reductive systems, other problems arise, such as the elimination of TiO_2 and the difficulty of controlling interfacial structure between copper thin films and the

* Corresponding author. Tel.: +886 35 731873; fax: +886 35 724727.
E-mail address: wtwhang@mail.nctu.edu.tw (W.-T. Whang).

0040-6090/$ - see front matter © 2008 Elsevier B.V. All rights reserved.
doi:10.1016/j.tsf.2007.12.166

underlying polyimide because of the ease of diffusion of copper in the polyimide. To improve Cu/PI films, a thin adhesion-promoting layer of such metals as Ni, Cr and Ti have been used to prevent Cu from diffusing into the PI substrate and also to promote interfacial adhesion [23–28]. Among these three metals, Ni is relatively environmentally harmless and cheap. Furthermore, it can be etched away by the same etchant as is used for copper. Therefore this investigation is the candidate for chemically developing Cu/PI systems with a thin Ni layer at the interface. Usually Ni electroless deposition is activated by Pd catalysts [29,30], which easily initiate the growth of Ni electroless deposition, but are expensive. Accordingly, a cheaper catalyst with high catalytic activity is urgently required to replace Pd materials.

This investigation will synthesize nickel nanoparticles as seeds (catalysts) and a Ni metal layer as an adhesion-promoting layer on the surface of a polyimide film using a wet chemical process. It can reduce the cost of the catalyst and simplify the process of coating the adhesion-promoting layer on the PI film. This study fully explores the formation of Ni-NPs and Ni layer. The following are adopted to investigate the structures and morphologies; attenuated total reflection FTIR spectroscopy (ATR-FTIR), X-ray diffraction spectroscopy (XRD), contact angle measurements, four-point probe conductivity measurements, atomic force microscopy (AFM), scanning electron microscopy (SEM), transmission electron microscopy (TEM), energy-dispersive X-ray spectroscopy (EDX) and the Scotch-tape test to determine adhesion between nickel and the polyimide films.

2. Experimental details

2.1. Materials

4, 4′-diaminodiphenylether (ODA, 98%) from Aldrich Chemical Co. was vacuum-dried for 3 h at 110 °C prior to use. Pyromellitic dianhydride (PMDA) from TCI was purified by recrystallization from a high-purity acetic anhydride and then dried in a vacuum oven at 120 °C for at least 14 h. Dimethylacetamide (DMAc) from Aldrich Chemical Co. was stored over molecular sieves prior to use. Potassium hydroxide (KOH), $NiSO_4 \cdot 6H_2O$, Sodium borohydride ($NaBH_4$), dimethylamine borane (DMAB) and sodium citrate all from TCI, and Lactic acid from Fluka were used as obtained.

2.2. Preparation of polyimide films

Poly(amic acid) (PAA) solutions were made by reacting equal molar amounts of diamine and dianhydride in solution (15% solid content (w/w) for ODA/PMDA in DMAc) under a nitrogen atmosphere. At beginning, ODA was firstly dissolved in DMAc, and then PMDA was added into the solution by five portions and it is better to ensure the completely dissolution of the prior portion before adding a fresh portion. After the dissolution of PMDA, the PAA solution was further stirred for 2 h at ambient temperature. The PI films were made by casting the PAA onto a dust free glass plate with a doctor blade, and then step-heated at 100 °C, 150 °C, 200 °C, 250 °C, 300 °C, 300 °C, and 350 °C, each step for an hour to form PI films with 40 μm thickness.

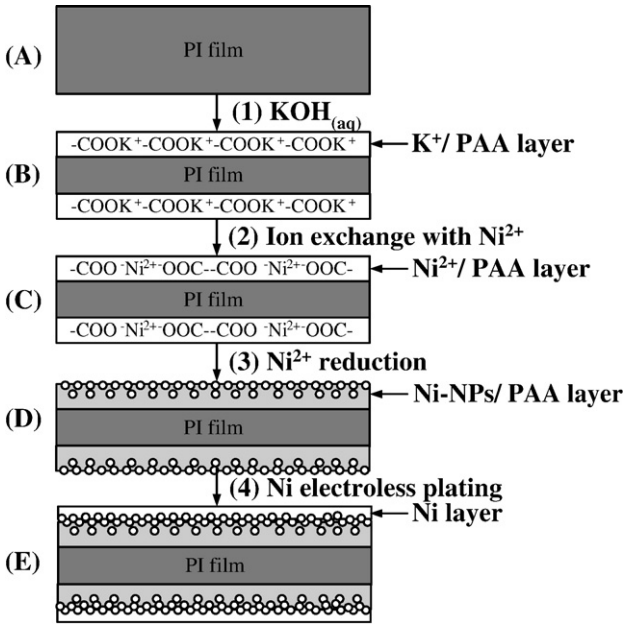

Fig. 1. Flow chart of formation of surface-nickelized polyimide films: (A) PI film: Pristine polyimide (B) K^+/PI film: K^+/PAA layer on PI film, (C) Ni^{2+}/PI film: Ni^{2+}/PAA layer on PI film, (D) Ni-NPs/PI film: Ni-NPs/PAA layer on PI film, (E) Ni/PI films: Ni/PAA layer on PI film.

2.3. Preparation of the surface-nickelized polyimide films

The preparation of nickel-coated conductive films was carried out according to the Fig. 1. The polyimide (PMDA-ODA) films were first immersed in a 1 M potassium hydroxide (KOH) aqueous solution at 50 °C for several min, followed by rinsing with deionized water. The PI films with the surface opening imide rings to exchange potassium ions with Ni^{2+} ions were immersed into a 50 mM nickel sulfate aqueous solution at 50 °C for several min, followed by rinsing with deionized water. The surface Ni^{2+} ions were then reduced in a sodium borohydride aqueous solution (0.2 g/100 ml deionized water) at 50 °C for 30 min to form Ni nanoparticles on PI surface. Theoretically, each borohydride ion can reduce four or two nickel ions: $4Ni^{2+} + BH_4^- + 8OH^- = B(OH)_4^- + 4Ni + 4H_2O$ or $4Ni^{2+} + 2BH_4^- + 6OH^- = 2Ni_2B + H_2 + 6H_2O$. The samples were rinsed with deionized water after reduction [4]. The nickel nanoparticles-seeded PI films were immersed in the electroless nickel bath (EN solution) to form thin Ni layers. The EN solution was prepared from a nickel stock solution and a DMAB solution with a 4/1 volumetric proportion. The nickel stock solution was composed of 40 g/L nickel sulfate, 20 g/L sodium citrate, and 10 g/L lactic acid in deionized water, and the DMAB aqueous solution was 1 g/L DMAB in deionized water. In alkaline and neutral solutions, the preceding chemical reaction of dimethylamine borane with OH^- ions could represent as:

$$(CH_3)_2NHBH_3 + OH^- = (CH_3)_2NH + BH_3OH^-.$$

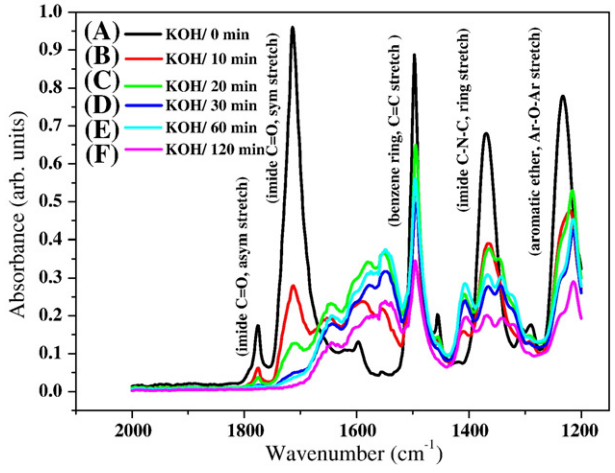

Fig. 2. ATR-FTIR absorption spectra of polyimide modified with KOH for different times.

DMAB has three active hydrogen atoms bonded to the boron, and theoretically can reduce three Ni^{2+} metal ions for each BH_3OH^- ion [31]:

$$BH_3OH^- + 3Ni^{2+} + 2H_2O = 3Ni + B(OH)_3 + 5H^+.$$

2.4. Measurements

FTIR absorption spectra were recorded by Perkin Elmer LEE-59 employing the attenuated total reflection (ATR) configuration. The ATR crystal, coated diamond crystal, was brazed into tungsten carbide disc. For sample of refractive index 1.5 at 1000 cm^{-1}, the depth of penetration was 2.0 μm. X-ray diffraction (XRD) spectra were obtained using a MacScience GIA model X-ray diffractometer. The equipment was operated with Cu Kα radiation, operating at 40 kV, 150 mA, with a scanning speed of 4° min^{-1} at steps of 0.02°. The contact angle and surface energy were measured and calculated by Dynamic Contact Analyzer FTA-200 from a contact angle test using two standard liquids: H_2O and CH_2I_2. The surface resistance of metalized PI films was measured using four-point probe (Napson RT-80/RG-80) and an average of the measured values was taken. The surface morphology changes of Ni-NPs/PI films were analyzed by atomic force microscopy (AFM) (SPI 3800N Probe Station, Seiko Instruments Inc., Japan) in tapping mode (silicon tips on silicon cantilevers with a spring constant 2 N/m and the set point about 0.8–0.9) in air. Scanning electron microscopy (SEM) with JEOL JSM-6500F was used to investigate the Ni surface on the polyimide films. X-ray photoelectron spectroscopy (XPS) measurements were obtained using an ESCA PHI 1600 spectrometer working in the constant analyzer energy mode with a pass energy 50 eV and Mg Kα (1253.6 eV) radiation as the excitation source. The XPS measurements were done at room temperature and pressure bellow 1.33×10^{-8} Pa. TEM was performed by employing a JEOL-2010 transmission electron microscope. The samples for TEM were microtomed with Leica Ultracut Uct into 90 nm thick slice and then moved onto a TEM copper grid with thick carbon layer. Elemental analysis was performed on an energy-dispersive X-ray (EDX) analyzer (OXFORD Instrument, Inc.) during TEM study. The accelerating voltage of TEM was 200 kV.

3. Results and discussion

Fig. 2 and Table 1 present the surface changes of polyimide modified with KOH, obtained using ATR-FTIR. In Fig. 2(A), the characteristic peaks of bare PI (PMDA/ODA) were clearly visible at ~1720, ~1780, ~1500, ~1380 and ~1230 cm^{-1}, corresponding to symmetric C=O stretching, asymmetric C=O stretching, benzene ring C=C stretching, imide ring C–N–C stretching and aromatic ether (Ar–O–Ar) stretching, respectively. Theoretically, after KOH treatment, the imide peak intensity at ~1720, ~1780, ~1380 and ~1230 cm^{-1} significantly changed but the benzene peaks at ~1500 cm^{-1} did not change. The obvious decline in the imide peak at ~1780 cm^{-1} was due to the opening of imide rings by KOH treatment. In Table 1, the peak height 0.9627 of the bare imide rings at 1720 cm^{-1} divided by the peak height 0.8876 of the unchanged benzene peak at 1500 cm^{-1} was 1.0846, which was set as the standard for a surface imide content of 100%. The peak height of the bare imide rings at 1720 cm^{-1} changed from 0.9627 to 0.2778 after 10 min KOH treatment. The relative surface imide content reduced to 45.7%, indicating that 54.3% of the imide rings were cleaved to form the carboxylic acids and amides, which were further converted to the more wettable CO_2^{-1} anions in aqueous KOH. After KOH treatment for 20 min, 30 min, 60 min and 120 min, the peak height of the residual imide characteristic peak had decreased from 18.4% to 4.6%, as shown in Table 1, suggesting that the proportion of cleaved imide rings increased from 81.6% to 95.4%. Extended KOH treatment could further increase the proportion of cleaved

Table 1
Dependence of relative surface imide content of PI films and surface morphology of Ni-NPs/PI films on treatment time with KOH

KOH/treatment time (min)	Peak height		H_{1720}/H_{1500}	Relative surface imide content (%)	Ra (surface roughness, nm)	D_{ave} (average Ni particle, nm)
	At 1720 cm^{-1} (imide peaks)	At 1500 cm^{-1} (benzene ring)				
(a) KOH/0	0.9627	0.8876	1.0846	100.0	0.89	–
(b) KOH/10	0.2778	0.5611	0.4951	45.7	23.90	269
(c) KOH/20	0.1298	0.6489	0.2000	18.4	11.64	131
(d) KOH/30	0.0520	0.4917	0.1058	9.8	14.30	161
(e) KOH/60	0.0396	0.5611	0.0706	6.5	10.00	113
(f) KOH/120	0.0172	0.3444	0.0499	4.6	5.99	–

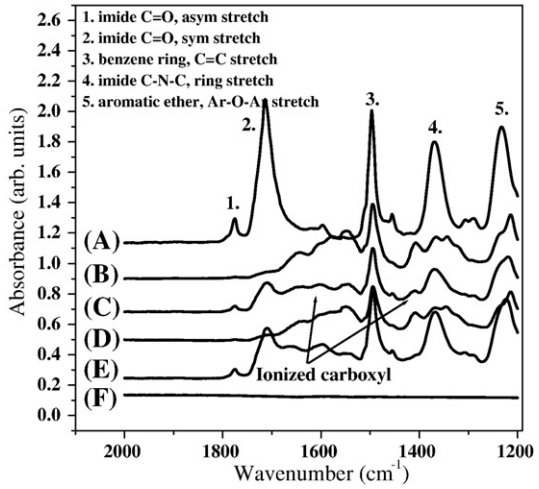

Fig. 3. ATR-FTIR absorption spectra of (A) pristine PI film, (B) K^+/PI films, (C) Ni^{2+}/PI film, (D) Ni-NPs/PI film, (E) Ni-NPs/PI film-310: Ni-NPs/PI film after annealing at 310 °C for 1 h, and (F) Ni/PI film.

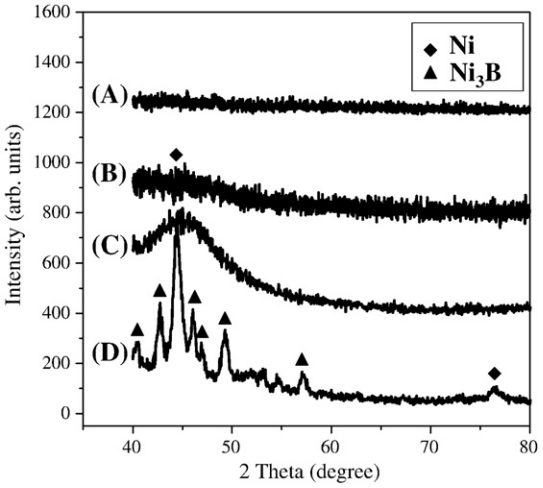

Fig. 4. XRD patterns of (A) pristine PI film, (B) Ni-NPs/PI film-110 (annealed at 110 °C for 1 h), (C) Ni/PI film-110 (annealed at 110 °C for 1 h), and (D) Ni/PI film-310 (annealed at 310 °C for 1 h).

imide rings, but it become warped and crooked at high cleaved imide content. The best PI film for following surface-nickelized treatments was obtained by treating KOH for 30 min, and it had the most wettable surface and a good appearance.

The chemical structures of the surface-nickelized process on PI films were characterized using an ATR-FTIR spectroscope, as displayed in Fig. 3. The characteristic peaks of imide groups in Fig. 3(A) at ~1780, ~1720 cm^{-1} and ~1380 cm^{-1} resulted from asymmetric C=O stretching, symmetric C=O stretching and imide ring C–N–C stretching, respectively. KOH treatment weakened the peak of the carbonyl stretching of imide rings, and produced new bands at 1500–1700 cm^{-1}, as shown in Fig. 3(B). Following ion exchange, a slight increase in peak intensity at ~1780 and ~1720 cm^{-1} with imide ring reformation, a slight enhancement in intensity at ~1680 cm^{-1} and complex features at around 1500–1600 cm^{-1} suggested that a number of coordination states coexist within the Ni^{2+} complexes, as presented in Fig. 3(C). The characteristic peak intensities of imide rings at ~1780 cm^{-1} and ~1720 cm^{-1} in Fig. 3(D) were lower, because the pH of aqueous $NaBH_4$ was 11 and this solution reopened surface imide rings. The reopened imide rings were closed by annealing at 310 °C for 1 h, as presented in Fig. 3(E). Fig. 3(F) shows no IR characteristic when more Ni was presented on the surface, because of the reflection or blocking of IR by the surface metal layer. Table 2 summarizes the clear changes in the peak height at 1720 cm^{-1} and the surface imide content following the full process. The peak height 0.9627 of the bare imide rings at 1720 cm^{-1} normalized with the peak height 0.8876 of the unchanged benzene peak at 1500 cm^{-1} is 1.0846, which value was set as the standard for a surface imide content of 100%. K^+/PI films had only a 9.8%

Table 2
Relative surface imide content on polyimide throughout process

Sample	Peak height		H_{1720}/H_{1500}	Relative surface imide content (%)
	At 1720 cm^{-1} (imide peaks)	At 1500 cm^{-1} (benzene ring)		
(a) PI films	0.9627	0.8876	1.0846	100.0
(b) K^+/PI films	0.0520	0.4917	0.1058	9.8
(c) Ni^{2+}/PI films	0.2004	0.4166	0.4810	44.3
(d) Ni-NPs/PI films	0.0284	0.3461	0.0821	7.6
(e) Ni-NPs/PI films-310	0.3325	0.5500	0.6045	55.7
(f) Ni/PI films	–	–	–	–

(a) PI films: Bare PI films.
(b) K^+/PI films: PI films treated with KOH aqueous solution (1 M, 30 min, 50 °C, pH=14).
(c) Ni^{2+}/PI films: K^+/PI films treated with $NiSO_4$ aqueous solution (50 mM, 30 min, 50 °C, pH=6).
(d) Ni-NPs/PI films: Ni^{2+}/PI films treated with $NaBH_4$ aqueous solution (30 min, 50 °C, pH=11).
(e) Ni-NPs/PI films-310: (d) Ni^{2+}/PI films are annealed at 310 °C for 1 h in vacuum.
(f) Ni/PI films: Ni-NPs/PI films treated with EN solution (10 min, 50 °C, pH=7).
–: the absorbance of functional group was not detected from ATR-FTIR.

Table 3
Contact angles and surface energies of pristine PI and different stages of modification of PI

Sample	Water	di-idomethane ($C_2H_4I_2$)	Surface energy (mN/m)
(a) PI films	75.5	41.1	39.1
(b) K^+/PI films	7.3	26.3	72.9
(c) Ni^{2+}/PI films	52.0	33.8	49.2
(d) Ni-NPs/PI films	76	32.6	43.4
(e) Ni/PI films	82.2	45.3	37.2
(f) Ni/PI films-110	86.3	53.0	32.9
(g) Ni/PI films-310	108.0	73.9	23.7

(a) PI films: Pristine PI films.
(b) K^+/PI films: PI films treated with KOH aqueous solution (1 M, 30 min, 50 °C).
(c) Ni^{2+}/PI films: K^+/PI films treated with $NiSO_4$ aqueous solution (50 mM, 30 min, 50 °C).
(d) Ni-NPs/PI films: Ni^{2+}/PI films treated with $NaBH_4$ aqueous solution (30 min, 50 °C).
(e) Ni/PI films: Ni-NPs/PI films treated with EN solution (10 min, 50 °C).
(f) Ni/PI films-110: annealing 110 °C for 1 h in vacuum.
(g) Ni/PI films-310: annealing 310 °C for 1 h in vacuum.

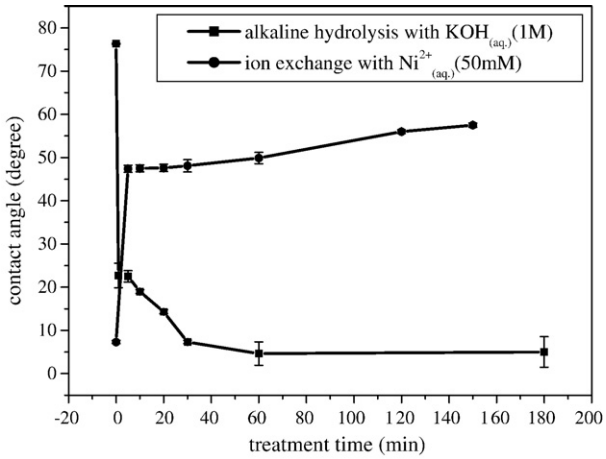

Fig. 5. Variation of contact angle of PI surface in the alkaline hydrolysis after treatment with KOH and then ion exchange with nickel ions.

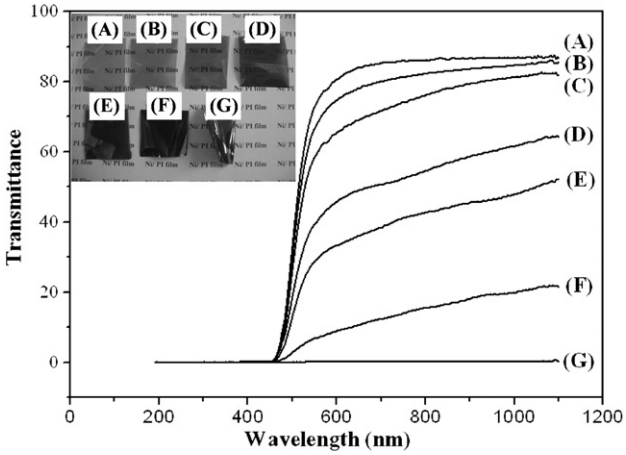

Fig. 6. Dependence of transparency and appearance of Ni-NPs/PI films (Ni-NPs/PI film treated with $KOH_{(aq)}$ for X min/$NiSO_{4(aq)}$ for 5 min/$NaBH_{4(aq)}$ for 30 min at 50 °C) on hydrolysis time (X min) during KOH treatment: (A) 0 min, (B) 5 min, (C) 10 min, (D) 20 min, (E) 30 min, (F) 60 min, (G) 120 min.

relative surface imide content in step (b). However, the relative surface imide content increased to 44.3% after ion exchange K^+ with Ni^{2+} at 50 °C for 5 min in step (c), since more imide rings were formed in the relatively acidic (pH 6) $NiSO_4$ solution. In the alkaline electroless Ni plating solution (pH 11), the surface imide content declined to 7.6% in step (d), but imidization at 310 °C for 1 h increased the surface imide content to 55.7% in step (e), because of ring closure during thermal treatment.

Fig. 4 presents the XRD patterns of the (a) PI films, (b) Ni-NPs/PI films (annealed at 110 °C for 1 h), (c) Ni/PI films (annealed at 110 °C for 1 h) and (d) Ni/PI films (annealed at 310 °C for 1 h). The pure PI film yielded no peak in Fig. 4(A). However, the XRD patterns of the sample (b) and (c), centered at 44.5°, revealed an amorphous hump, which may have originated from the amorphous phase of nickel particles. After the samples were annealed at 310 °C for 1 h, two peaks of Ni were observed at $2\theta = 44.5°$ and 76.4°, and six peaks from Ni_3B were presented at $2\theta = 40.4°$, 42.7°, 46°, 47°, 49.3° and 57.3°, suggesting that annealing at 310 °C increased the ordering of the packing of Ni and Ni_3B.

Table 4
Surface resistances and tape adhesion testing results of bare PI and metalized PI

Sample (mode: V/I)	Surface resistance (Ω/cm^2)	Tape adhesion performance per ASTM D3359-95 [32]
(a) PI films	–	No test
(b) Ni-NPs/PI films-d	15.88 M	No pass
(c) Ni-NPs/PI films-a	–	No pass
(d) Ni/PI films	6.44	Pass
(e) Ni/PI films-110	3.45	Pass
(f) Ni/PI films-310	0.83	Pass
(g) Ni/Cu/Ta/SiO2/Si-300	0.2	No test

(a) PI films: Bare PI films.
(b) Ni-NPs/PI films-d: directly measured after modified.
(c) Ni-NPs/PI films-a: measured after modified for over 1 day.
(d) Ni/PI films: without annealing.
(e) Ni/PI films-110: Ni/PI films annealed 110 °C for 1 h in vacuum.
(f) Ni/PI films-310: Ni/PI films annealed 310 °C for 1 h in vacuum.
(g) Ni/Cu/Ta/SiO_2/Si-300: NiB film formed on Cu (100 nm)/Ta (30 nm)/SiO_2 (500 nm)/Si substrate and annealed at 300 °C [33].
–: the surface resistance was not detected from four-point probe.

Table 3 displays the contact angles and surface energies of bare PI and modified PI in different steps, measured using water and di-idomethane. The contact angle of the PI film with water was 75.5°. KOH treatment substantially reduced the water contact angle of the K^+/PI film to 7.3°, because more imide rings cleaved to form wettable CO_2^- anions. Ion exchange with Ni^{2+} increased the water contact angle of the Ni^{2+}/PI film to 52°, because of the acidity of the $NiSO_4$ solution. The acidic solution caused the formation of more imide rings in this step, as presented in Fig. 3(C). In the fourth step, when the Ni-NPs were

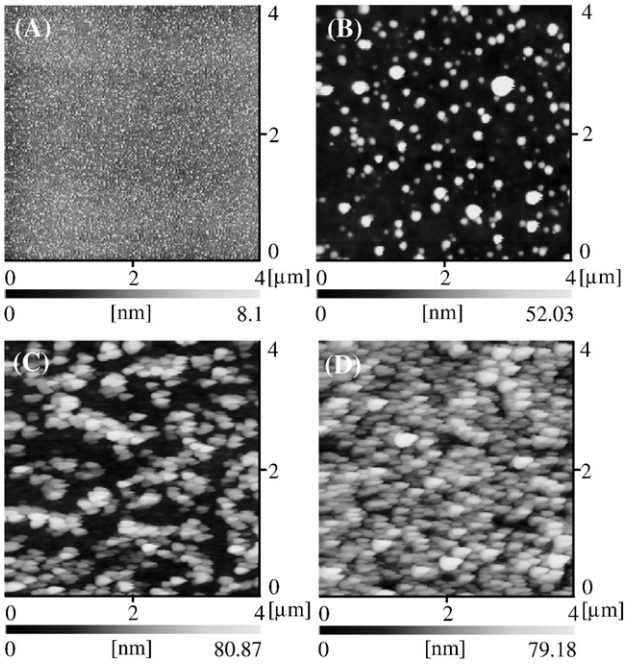

Fig. 7. AFM photographs of nanostructured Ni-NPs/PI films (Ni-NPs/PI film treated with $KOH_{(aq)}$ for 10 min/$NiSO_{4(aq)}$ for 5 min/$NaBH_{4(aq)}$ for 30 min at 50 °C) for various hydrolysis times with KOH treatment: (A) 0 min, (B) 5 min, (C) 30 min, (D) 60 min. (left: top-view diagram; range of z is 200 nm; right: phase diagram, range of z is 200°).

formed by reducing Ni^{2+} to Ni-NPs, the contact angle of the surface increased markedly to 76°, which is presumed the result from the integral effects of Ni-NPs and bare PI films. Finally, when the nanoseeds were used to grow nickel films in EN solution, the contact angle increased further to 82.2° and the surface energy decreased to 37.2 (mN/m). In spite of the low relative surface imide content, the high relative surface wettability and the water contact angle unexpectedly increased, because the Ni-NPs surface is rough and exhibits a partial lotus effect. When the Ni/PI films were thermally aged at 110 °C and 310 °C respectively, the water contact angles were higher and the surface energy lower after the high-temperature treatment, the high-temperature aging reformed the imide ring from the polyamic acid and densified the Ni layer more effectively, as shown in Fig. 4.

Fig. 5 plots the optimum treatment time with KOH and $NiSO_4 \cdot 6H_2O$ aqueous solution at 50 °C. When PI films were modified with KOH for 0, 2, 4, 6, 8, 10, 15, 20, 30, 60 and 180 min, the contact angle with water sharply decreased in the first 4 min. The decline slowed down from 4 min to 30 min. Finally, the contact angle remained constant from 30 min to 180 min. However, when ring-opened PI films were ion-exchanged with $NiSO_4 \cdot 6H_2O$ aqueous solution for 0, 5, 10, 20, 30, 60, 120 and 150 min, the surface contact angle rapidly increased from 9.7° to 47.9°, and then slowly increased from 47.9° to 57.5°, revealing that the Ni^{2+} ion exchange rate is very high. Therefore, the optimum treatment time with $NiSO_4 \cdot 6H_2O$ at 50 °C was 5 min.

Table 4 presents the surface resistances and tape adhesion results for pristine PI and metalized films, measured using a four-point probe and the ASTM D3359-95 method [32]. The surface resistance of pristine PI was too high to be detected by the four-point probe instrument. The value for the Ni-NPs/PI film (directly measured after the reduction of nickel ions) was lower, at 15.88 $M\Omega/cm^2$. However, after one day, the surface resistance of the modified Ni-NPs/PI was undetectable. The Ni-NPs/PI film with high surface energy was prone to be oxidized, and became less conductive, as shown in Fig. 8(G). In this figure, (a) the Ni-NPs/PI film-d was measured directly after the reduction of nickel ion and (b) the Ni-NPs/PI film-a was

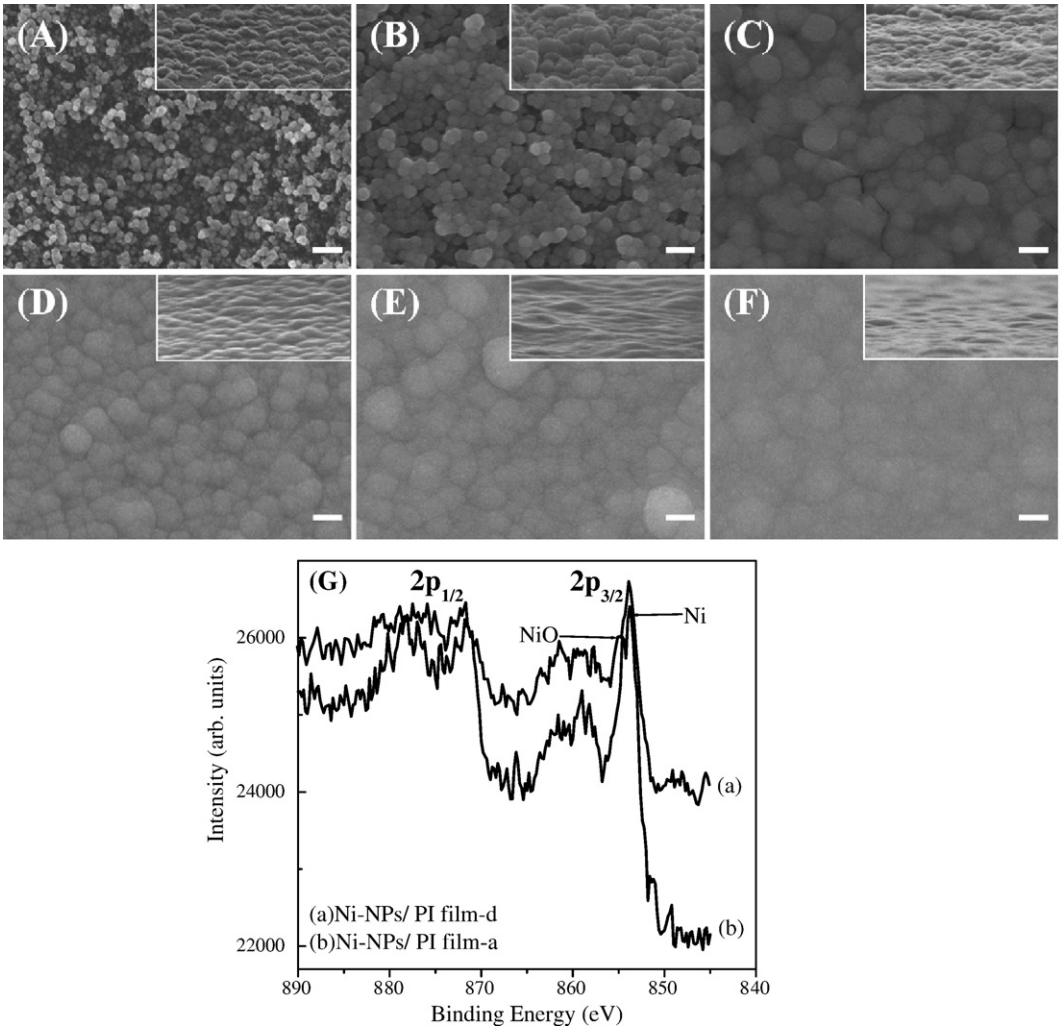

Fig. 8. FE-SEM images of electroless-plated nickel on Ni-NPs/PI films (Ni-NPs/PI film treated with $KOH_{(aq)}$ for 30 min/$NiSO_{4(aq)}$ for 5 min/$NaBH_{4(aq)}$ for 30 min at 50 °C) at 50 °C for (A) 0 min, (B) 2 min, (C) 4 min, (D) 6 min, (E) 10 min, (F) 15 min. White bars represent 200 nm. (left: top-view, right: tilt 45°-view). XPS spectra of Ni-NPs/PI films. (a) Ni-NPs/PI film-d (measured directly), (b) Ni-NPs/PI film-a (measured after one day).

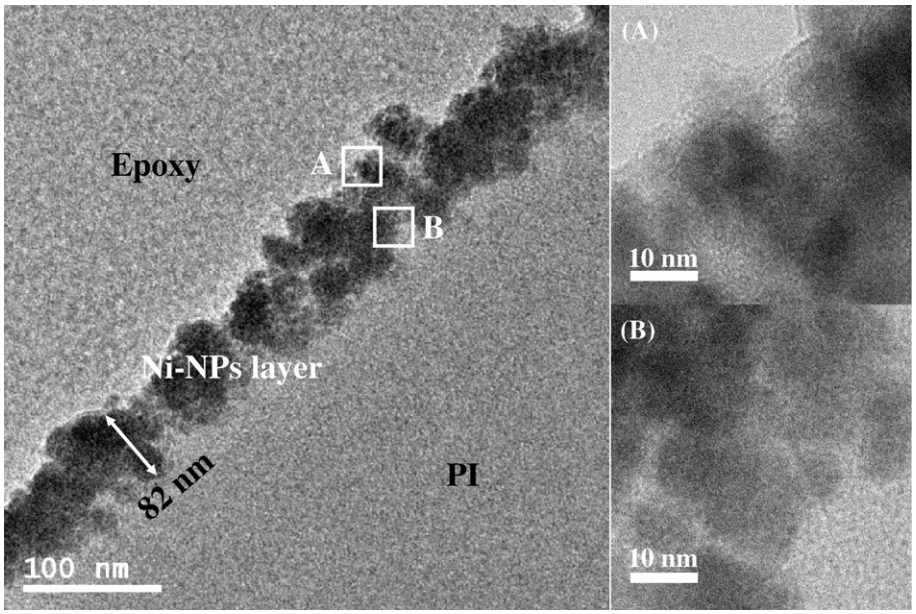

Fig. 9. TEM photographs of cross section of Ni-NPs/PI film (Ni-NPs/PI film treated with $KOH_{(aq)}$ for 10 min/$NiSO_{4(aq)}$ for 5 min/$NaBH_{4(aq)}$ for 30 min at 50 °C). The bar represents 100 nm. The A-area and B-area are outside and inside the Ni-NPs layer, respectively.

measured after one day using XPS. The NiO peak at 864 eV was clearly observed one day after that appeared from (a) Ni-NPs/PI film-d. Ni/PI films have higher conductivity, but sampled that were annealed at different temperature had different conductivities. The surface resistances of Ni/PI films (without annealing), Ni/PI films (annealing 110 °C/1 h) and Ni/PI films (annealing 310 °C/1 h) were 6.44 Ω/cm^2, 3.45 Ω/cm^2 and 0.83 Ω/cm^2, respectively. The higher annealing temperature corresponded to lower surface resistance. This relation is explained by the fact that high annealing temperature favored the crystallization of Ni and the restructuring of the grain boundary, as evidenced by Fig. 4(B)–(D). The surface resistance of Ni-B following electroless deposition [32] was of the same order of magnitude as observed experimentally herein. Tape adhesion test results demonstrated that no Ni-NPs/PI film passed this test, but all of the Ni/PI films passed the Scotch-tape (ASTM D3359-95: with Scotch 610) the interfacial adhesion test between Ni and PI without any isolated spot or pit.

Fig. 6 shows the transparency and appearance of Ni-NPs/PI films (Ni-NPs/PI film treated with $KOH_{(aq)}$ for X min/$NiSO_{4(aq)}$ for 5 min/$NaBH_{4(aq)}$ for 30 min at 50 °C) with various KOH treatment times ((A) 0 min, (B) 5 min, (C) 10 min, (D) 20 min,

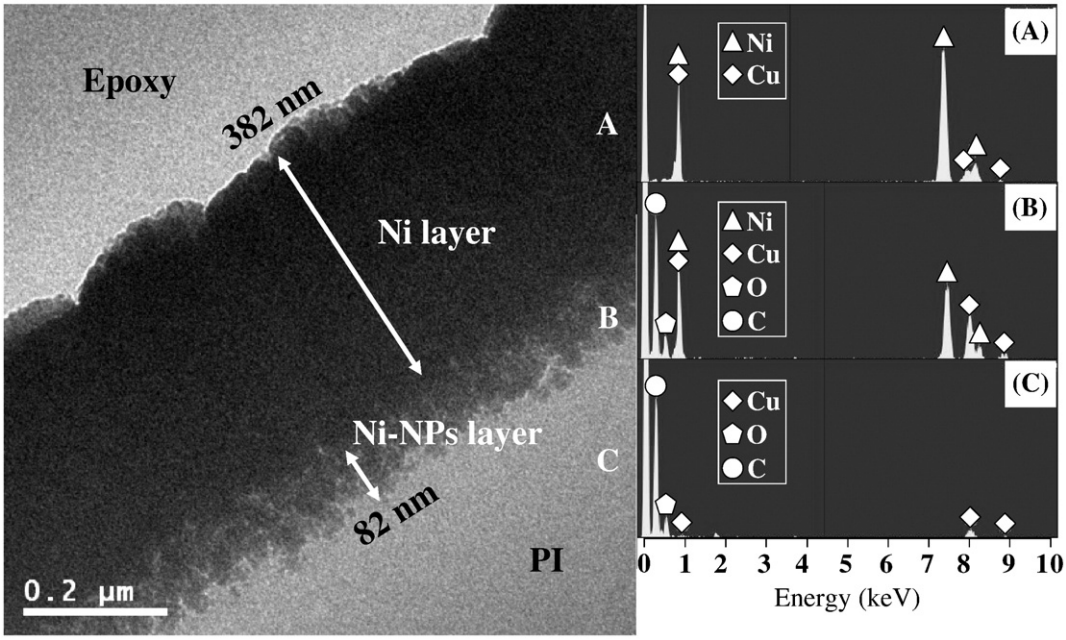

Fig. 10. TEM photographs (left) and EDX analysis (right) of cross section of surface-nickelized PI films: A–the Ni layer, B–the Ni-NPs layer, C–PI film.

(E) 30 min, (F) 60 min, (G) 120 min). In Fig. 6(A), the pristine PI film is yellow–brown and very transparent. In Fig. 6(B)–(F), the Ni-NPs distributed on PI films were black and became darker as the KOH treatment time increased. In Fig. 6(F) and (G), the samples were warped and changed color from black to silver. Samples (B)–(G) of Ni-NPs/PI films easily underwent electroless deposition.

Fig. 7 displays AFM topview diagrams of the nanostructured Ni-NPs/PI films for different KOH treatment times; (A) 0 min, (B) 5 min, (C) 30 min, (D) 60 min. In Fig. 7(A) the pristine PI film was smooth and had a uniform surface topography. After KOH treatment for 5 min, a few of nanosized nickel particles of size 85 nm were present, as observed in Fig. 7(B). As the KOH treatment time increased, more Ni nanoparticles formed on the surface of the PI films. After a KOH treatment time of 30 min or 60 min, as display in Fig. 7(C)–(D), the Ni-NPs were more uniform and denser. Table 1 presents that, the dependence of the surface roughness and average Ni particle size of Ni-NPs/PI films on the KOH treatment time ((a) 0 min, (b) 10 min, (c) 20 min, (d) 30 min, (e) 60 min, (f) 120 min), as determined using AFM. In Table 1(a), the surface roughness was 0.89 nm and no Ni-NP was present on PI. In Table 1(b)–(e), the surface roughness was 23.90, 11.64, 14.30 and 10.00 nm, respectively, and the average particle sizes of Ni-NPs were 269, 131, 161 and 113 nm, respectively. In Table 1(f), the surface roughness was 5.99 nm and the surface of the PI film was uniformly covered with Ni particles, which formed a continuous Ni layer.

Fig. 8 presents the surface topographies of electroless nickel layers that were grown on Ni-NPs/PI films (Ni-NPs/PI film treated with $KOH_{(aq)}$ for 30 min/$NiSO_{4(aq)}$ for 5 min/$NaBH_{4(aq)}$ for 30 min at 50 °C), obtained using FE-SEM. All scale bars in Fig. 8(A)–(F) were 200 nm, and the dipping times in EN solution were 0, 2, 4, 6, 10, 15 min, respectively. Fig. 8(A) displays the original Ni-NPs deposited on modified PI surface, where the sizes of the spherical nickel nanoparticles were approximately 50 nm, which size is the same as in Fig. 7(C). Dipping in EN solution at 50 °C for 2 min increased the size of the Ni-NPs from 50 nm to 100 nm, as shown in Fig. 8(B). Electroless nickel treatment at 50 °C for 4, 6 and 10 min increased the particle size had from 150 nm to 300 nm, and the surface morphology of the Ni/PI films in Fig. 8(C)–(E) was denser and smoother. Finally, after it had been treated for 15 min, the nickel film had a flat and smooth surface and was difficult to identify the particle sizes and grain boundaries of the nickel particles in Fig. 8(F).

Figs. 9 and 10 present cross-sectional TEM images of the Ni-NPs/PI film and the Ni/PI film, respectively. The Ni-NPs/PI film was treated with $KOH_{(aq.)}$ at 50 °C for 5 min, underwent ion exchange with $NiSO_4 \cdot H_2O_{(aq.)}$ at 50 °C for 5 min, and was then reduced by $NaBH_{4(aq.)}$ at 50 °C for 30 min. The pre-treatment of the Ni/PI film in Fig. 10 was the same as that in Fig. 9 and the EN solution was then used to increase the thickness of the nickel layer at 50 °C for 10 min without any annealing. Fig. 9 shows that the thickness of the Ni-NPs layer was 82 nm. Fig. 9(A) and (B) are TEM images of the outside and the inside of the Ni-NPs layer, respectively. Fig. 9(A) and (B) indicate that Ni-NPs were discontinuous in the layer with particle sizes of 10 nm. In Fig. 10, the three layers in this Ni/PI film were the Ni layer, the Ni-NPs layer and the PI layer in that order. The TEM photographs show that in the Ni layer, the metal was continuous, but in the Ni-NPs layer, Ni-NPs were dispersed in the polymer and interlocked therewith. The thickness of the Ni layer was 382 nm and that of the Ni-NPs layer was 82 nm. EDX analysis confirmed the structure of these three layers, as shown in Fig. 10. The EDX intensity of copper signals for each layer was from the TEM copper grid, and the oxygen and carbon signals were from PI. Accordingly, the EDX results verified that the A-area was composed of electroless-plated nickel; the B-area was composed of Ni-NPs and polymer, and the C-area comprised PI without Ni.

4. Conclusion

Conductive Ni/PI films are fabricated using a fully chemical solution-based process without Pd, and adhere strongly between polyimide and nickel phases. Unlike traditional processes, this process does not require the use of Pd catalyst. Additionally, it is convenient for preparing conductive Ni on one or both sides of PI films. Ni-NPs can be homogeneously distributed on the PI surface after reduction by aqueous $NaBH_4$. After electroless plating, the Ni layer exhibits excellent interfacial adhesion on the PI surface and passes the Scotch-tape test. The interlocking of the nickel layer with the PI layer may contribute to the interfacial adhesion. Measurements of surface conductivity reveal that the surface resistance of Ni-NPs is $1.6 \times 10^7\ \Omega/cm^2$, but that of Ni/PI film is 0.83 Ω/cm^2 after EN treatment and heating at 310 °C for 1 h. The described method is good for electroplate metal onto nickelized PI surfaces to apply on flexible electronics.

Acknowledgment

The authors would like to acknowledge the financial support of the National Science Council through project NSC 95-2221-E-009-121, and Taimide Technology Company.

References

[1] J.D. Rancourt, G.M. Porta, T.L. Taylor, Thin Solid Films 158 (1988) 189.
[2] M.M. Ellison, L.T. Taylor, Chem. Mater. 6 (1994) 990.
[3] J.B. Ma, J. Dragon, W. Van Derveer, A. Entenberg, V. Lindberg, M. Anschel, D.Y. Shih, P. Lauro, J. Adhes. Sci. Technol. 9 (1995) 487.
[4] C.A. Chang, J.E. Balgin, A.G. Schrott, K.C. Lin, Appl. Phys. Lett. 51 (1987) 103.
[5] N. Inagaki, S. Tasaka, K. Hibi, J. Adhes. Sci. Technol. 8 (1994) 395.
[6] G. Rozovskis, J. Vinkevicius, J. Jaciauskiene, J. Adhes. Sci. Technol. 10 (1996) 399.
[7] Y. Nakamura, Y. Suzuki, Y. Watanabe, Thin Solid Films 290/291 (1996) 367.
[8] A.M. Ektessabi, S. Hakamata, Thin Solid Films 377/378 (2000) 621.
[9] P.C. Chiang, W.T. Whang, S.C. Wu, K.R. Chuang, Polymer 45 (2004) 4465.
[10] R.E. Southward, D.W. Thompson, A.K. St. Clair, Chem. Mater. 9 (1997) 501.
[11] T. Sawada, S. Ando, S. Sasaki, Appl. Phys. Lett. 74 (1999) 938.
[12] S. Ikeda, K. Akamatsu, H. Nawafune, J. Mater. Chem. 11 (2001) 2919.
[13] K. Akamatsu, S. Ikeda, H. Nawafune, Langmuir 19 (2003) 10366.

[14] K. Akamatsu, S. Ikeda, H. Nawafune, S. Deki, Chem. Mater. 15 (2003) 2488.
[15] S. Ikeda, K. Akamatsu, H. Nawafune, T. Nishino, S. Deki, J. Phys. Chem. B 108 (2004) 15599.
[16] K. Akamatsu, S. Ikeda, H. Nawafune, H. Yanagimoto, J. Am. Chem. Soc. 126 (2004) 10822.
[17] Z. Wu, D. Wu, S. Qi, T. Zhang, R. Jin, Thin Solid Films 493 (2005) 179.
[18] Z. Wu, D. Wu, W. Yang, R. Jin, J. Mater. Chem. 16 (2006) 310.
[19] R.T. Richard, Langmuir 12 (1996) 5247.
[20] E.S. Lori, M. Anthony, R.T. Richard, Langmuir 16 (2000) 4706.
[21] R.T. Richard, Langmuir 19 (2003) 5763.
[22] C. Ailger, R. Stadler, Macromolecules 23 (1990) 2097.
[23] N.J. Chou, C.H. Tang, J. Vac. Sci. Technol. A2 (1984) 751.
[24] F.S. Ohuchi, S.C. Freilich, J. Vac. Sci. Technol. A4 (1986) 1039.
[25] J.L. Jordan, P.N. Sanda, J.F. Morar, C.A. Kovac, F.J. Himpsel, R.A. Pollack, J. Vac. Sci. Technol. A4 (1986) 1046.
[26] L.J. Atanasoska, S.G. Anderson, H.M. Meyer III, Z. Lin, J.H. Weaver, J. Vac. Sci. Technol. A5 (1987) 3325.
[27] F. Faupel, R. Willecke, A. Thran, Mater. Sci. Eng., R 22 (1998) 1.
[28] E. Kondoh, Thin Solid Films 359 (2000) 255.
[29] T.C. Wang, B. Chen, M.F. Rubner, R.E. Cohen, Langmuir 17 (2001) 6610.
[30] T.C. Wang, M.F. Rubner, R.E. Cohen, Chem. Mater. 15 (2003) 299.
[31] T. Homma, A. Tamaki, H. Nakai, T. Osaka, J. Electroanal. Chem. 559 (2003) 131.
[32] ASTM D3359-95 standard method for measuring adhesion by tape test, Annual Book of ASTM Standards, vol. 06.01.
[33] T. Osaka, N. Takano, T. Kurokawa, T. Kaneko, K. Ueno, Surf. Coat. Technol. 169/170 (2005) 124.